Available online at www.sciencedirect.com
ScienceDirect
Journal of Power Sources 161 (2006) 1076–1083
JOURNAL OF POWER SOURCES
www.elsevier.com/locate/jpowsour

Experimental investigation of coupling phenomena in polymer electrolyte fuel cell stacks

Marco Santis, Stefan A. Freunberger, Matthias Papra [1], Alexander Wokaun, Felix N. Büchi *

Electrochemistry Laboratory, Paul Scherrer Institut, CH-5232 Villigen PSI, Switzerland

Received 27 March 2006; received in revised form 5 May 2006; accepted 1 June 2006
Available online 18 July 2006

Abstract

Propagation of performance changes to adjacent cells in polymer electrolyte fuel cell stacks is studied by means of voltage monitoring and local current density measurements in peripheral cells of the stack. A technical fuel cell stack has been modified by implementing two independent reactant and coolant supplies in order to deliberately change the performance of one cell (anomalous cell) and study the coupling phenomena to adjacent cells (coupling cells), while keeping the working conditions of the later cell-group unaltered.

Two anomalies are studied: (i) air starvation and (ii) thermal anomaly, in a single anomalous cell in the stack and their coupling to adjacent cells. The results have shown that anomalies inducing considerable changes in the local current density of the anomalous cell (such as air starvation) propagate to adjacent cells affecting their performance. The propagation of local current density changes takes place via the common bipolar plate due to its finite thickness and in-plane conductivity. Consequently, anomalies which do not strongly influence the local current density distribution (such as a thermal anomaly under the studied working conditions) do not propagate to adjacent cells.

Keywords: Fuel cell stacks; Propagation of anomalies; Electrical coupling; Current density distribution

1. Introduction

A polymer electrolyte fuel cell stack (PEFC stack) usually comprises of a number of single cells, all connected electrically in series with a parallel supply of reactant gases and coolant. In an ideal fuel cell stack, each of the components of the repeating unit in the stack, i.e. every single cell, as well as the operating conditions for all cells should be identical throughout the complete stack. Integral stack performance would then be the sum of the equal stand-alone performances of all cells.

However, in a real stack, although the working conditions are set to provide each individual cell equally with reactants and coolant, location in the stack as well as small structural differences due to manufacturing tolerances may create a non-identical distribution of operating conditions at single cell level. Differences in water management (e.g. stochastic accumulation of liquid water), under-average reactant supply (below the set stoichiometries for the stack) and/or insufficient coolant supply are some of the possible non-uniformities that can be encountered at single cell level, translating into performance differences, very often not of a single cell only, but of a group of cells located adjacent to each other. So why do cells in a stack show sometimes a coupled behavior?

To address this question, investigations at stack level are needed. Classically, in order to ensure proper operation of the complete fuel cell stack, performance of each individual cell is monitored by measuring its voltage. An unexpected decrease in cell voltage is then an indication for anomalous behavior. Nevertheless, measuring cell voltage provides only limited information about the effects giving rise to performance changes and endows practically no particulars about coupling phenomena between individual cells.

Locally resolved investigations of current density distribution [1–4], impedance spectroscopy [5], liquid water distribution [6],

* Corresponding author. Tel.: +41 56 3102411; fax: +41 56 3104415.
E-mail addresses: marco.santis@psi.ch (M. Santis), stefan.freunberger@psi.ch (S.A. Freunberger), matthias.papra@hoppecke.com (M. Papra), alexander.wokaun@psi.ch (A. Wokaun), felix.buechi@psi.ch (F.N. Büchi).
[1] Present address: HOPPECKE Batterien GmbH & Co. KG, Bontkirchener Str. 1, D-59929 Brilon, Germany.

0378-7753/$ – see front matter © 2006 Elsevier B.V. All rights reserved.
doi:10.1016/j.jpowsour.2006.06.007

and gas composition analysis [7] among others, provide information to understand local phenomena and performance in fuel cells. These investigation techniques are well established at single cell level; however, local diagnostic work at fuel cell stack level has not yet been as widely performed. Recently, Kim et al. presented some experimental and modeling work on the electrical coupling of cells in a stack [8]. They studied two types of anomalies: a partially inactive cell and a resistive bus plate with limiting in-plane conductivity. However, for their investigations they monitored only the individual cell voltages.

In the present work, measurement of local current density in adjacent cells in a stack has been implemented to study two other types of anomalies: (i) air starvation at single cell level and (ii) thermal anomaly, as encountered at peripheral cells in a stack.

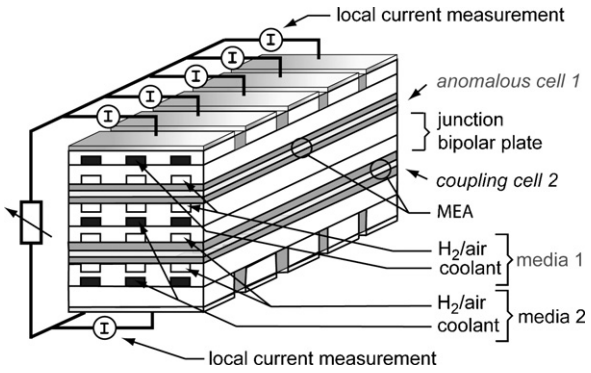

Fig. 1. Simplified scheme of a two-cell (1 + 1) stack with independent media supplies and location of local current density measurement at the stack periphery.

2. Experimental

2.1. Measurement method and operating conditions

For the purpose of the presented studies, two- and three-cell technical stacks, modified by implementing a second, independent reactant and coolant supply, were used. The cells in the stack were therefore separated in two groups, each cell-group having an independent media supply, allowing for operation at different conditions with respect to stoichiometry and/or dew point of the reactants and inlet coolant temperature. The modified stacks are denoted as 1 + 1 and 1 + 2 stacks, respectively. For each operating condition the voltage of the cells in the stack was monitored while the current density distribution was recorded simultaneously in the peripheral cells of the stack.

Fig. 1 shows a scheme of a 1 + 1 stack with independently controlled media supplies for the individual cells as well as the location of the local current density measurement at the stack periphery. For the sake of comprehensibility, in Fig. 1 a stack with a linear geometry and symmetrical segmentation is shown. The actual flow field geometry and segmentation are shown in Fig. 2. In the modified stack, the two individual cells are connected electrically and thermally via the junction bipolar plate, which also separates the two media streams. For emulation of anomalies in the stack, the operating conditions in the upper cell (anomalous cell) can be independently varied, while keeping them constant in the second cell-group (coupling cells). The cells are cooled from both sides of the membrane electrode assemblies (MEA). The coolant temperature in the outer-part of the anomalous cell can be controlled independently as it belongs to a separate coolant supply, while cooling in the junction bipolar plate is part of the second coolant loop belonging to the coupling cell(s).

Table 1 gives an overview of the investigated cases of air starvation and thermal anomalies realized with 1 + 1 and 1 + 2-cell stacks.

The cells were operated under the following standard conditions (exceptions given in Table 1): cell temperature of $T_c = 70\,^{\circ}C$ (water inlet and outlet temperature difference of less than 1 °C), gas outlet pressures of $p = 2.0$ bar (abs), hydrogen and air stoichiometries of $\lambda_{H_2} = 2.0$ and $\lambda_{air} = 4.0$, respectively, and hydrogen and air dew points of $T_d = 70\,^{\circ}C$. The reactant gases were fed fully humidified in order not to induce humidification related changes in the current density distribution. The reported measurements were carried out in constant current mode at an average current density $\bar{j}$ of 390 mA cm^{-2} (corresponding to 80 A total stack current).

The stacks were built using technical cells with an active area of 205 cm^2 [9]. Fig. 2 shows the design of the cell with the air

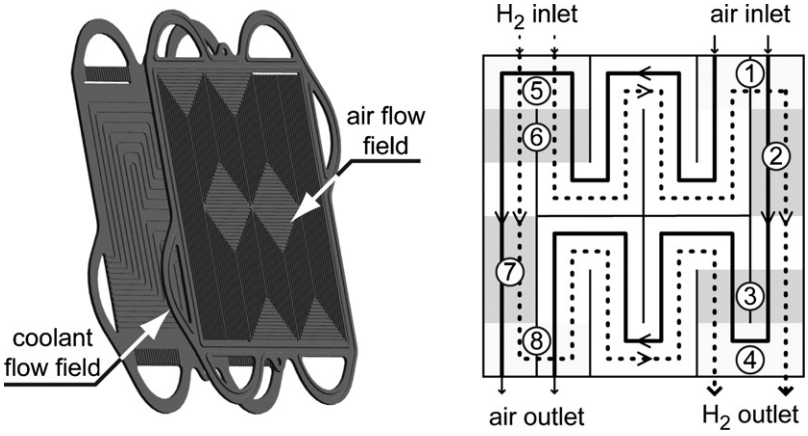

Fig. 2. (left) Two-part, water-cooled bipolarplate with the air and part of the cooling flow fields shown. (right) Location of the individual segments and schematic paths of air and hydrogen in the plate.

Table 1
Overview of the studied cases with the status and working conditions of the cells in the indicated stacks

Case	Stack	Anomalous cell	Emulated anomaly	Operating condition varied		
				Cell 1	Cell 2	Cell 3
0	1 + 1	1 and 2	Air starvation	λ_{air}	λ_{air}	–
1	1 + 1	1	Air starvation	λ_{air}	All constant	–
2	1 + 2	1	Air starvation	λ_{air}	All constant	All constant
3	1 + 1	1	Thermal losses	Coolant temperature	All constant	–

and part of the coolant flow fields, as well as the position of the individual segments for local current density measurement over the active area. The segmentation of the active area was chosen in order to study local current density at different lengths along the reactants path and especially at the reactants in- and outlets. Hydrogen and air flow in a meander-type way in two streams over the active area. Cooling of the cells is realized inside of the two-part bipolar plates. For a better overview only the schematic air and hydrogen paths are shown in Fig. 2. A more detailed description of the cell design can be found in [10,11].

For mapping of the current density distribution along the air channel length, the segments 1, 2, 4, 5, 7 and 8 are used. The midpoints of these segments are located at 3%, 11%, 34%, 66%, 89% and 97% from the beginning of the air path, respectively. The segments 3 and 6 are used in addition, when mapping local current along the hydrogen channel length.

Measurement of local current density was realized by a semi-segmented plate principle [2]. The active area was divided in nine segments, eight small segments of 10.7 cm^2 (A_{SS}) and one big central segment of 119.4 cm^2 (A_{CS}). Each segment of the semi-segmented cathode and anode plates in the first and last cells of the stack, respectively, is connected to separate copper rods, in which the current is measured by means of Hall sensors with an accuracy of +1 mA cm^{-2}.

The resistance of the connection between individual segments (R_{SS} for the small segments and R_{CS} for the big central segment) and the common node needs to be as low as possible in order to minimize the influence of the additional resistance on the current distribution pattern [12]. Since the active area of the cell is not symmetrically segmented, the inverse ratio of the areas and connection resistances for the small and for the big segments has to be kept constant in order to keep the same voltage drop in all connections. The resistance of the connections of the eight small segments is thus dictated by the minimum achievable resistance of the connection to the big segment by the equation $R_{SS} = (A_{CS}/A_{SS})R_{CS}$. The presented measurements were made with a connection to the big segment of 0.05 mΩ (limited by spatial issues in the experimental setup); the connections for the small segments were therefore set to 0.56 mΩ by adjusting the length of the respective copper rods.

With the given resistances, the measurements presented in this work have a deviation of less than ±4% from the values obtained by extrapolation to zero external resistance [12].

The electrical parameters of the cell were controlled using an electronic load (Höcherl and Hackl Series DS). Gas flow rates and pressure of the reactant gases were controlled using electronic mass flow controllers (Brooks®) and backpressure regulators (Brooks®), respectively. These controllers and the electronic load were interfaced to a personal computer.

2.2. Cell components

The design of the bipolarplate has been shown in Fig. 2. The two-part bipolar plates were fabricated by a pressure molding process using SGL BMA5-type graphite (SGL, Meitingen, Germany). The in-plane and trough-plane conductivities of the plate-material are 100 and 20 S cm^{-1}, respectively. The two-part bipolar plate has a thickness of 3.1 mm and the active area a size of 141.5 mm × 145 mm.

The membrane electrode assemblies were prepared using Nafion® 112 membranes and commercial E-Tek Elat A7 gas diffusion electrodes. Both gas diffusion electrodes, at anode and cathode, had a uniform catalyst loading of 0.6 mg cm^{-2} and Nafion® impregnation of 0.6 mg cm^{-2}.

3. Results and discussion

3.1. Case 0—verification of experimental setup

For the verification of the experimental setup a base case experiment (case 0, see Table 1) with a two-cell stack (1 + 1) was carried out monitoring cell voltage and current density distribution in both cells. In the 1 + 1-cell stack, both cells can be operated as stand-alone cells with respect to reactant and coolant supply. Consequently, when the operating conditions in both cells are varied equally, changes in performance are expected to be identical for both cells.

For case 0 an air starvation anomaly throughout the whole stack was emulated by reducing air stoichiometry in the two independent air supply streams simultaneously. Fig. 3 shows, for both cells, changes in cell voltage as a function of the air stoichiometry (a) and net variations in current density as a function of the normalized air channel length for the given air stoichiometries (b). In case 0, cells 1 and 2 are denoted as anomalous cells. The changes in cell voltage and local current density are shown with reference to values obtained at an air stoichiometry of 4.0 in both cells.

As it can be seen in Fig. 3, changes in cell voltage as well as in current density distribution in both cells are practically identical, validating the experimental setup. Reduction of air stoichiometry translates into a decrease in cell voltage. This is on the one hand due to the reduced average oxygen partial pressure (Nernstian thermodynamic effect), which in addition also results

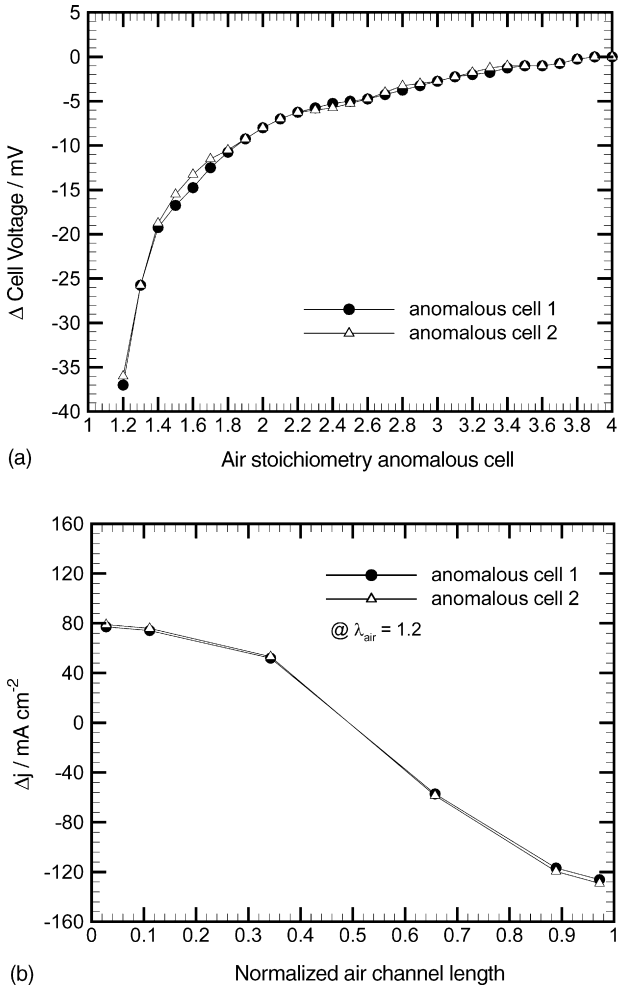

Fig. 3. 1 + 1-Cell stack. (a) Changes in cell voltage of cells 1 and 2, plotted as a function of the air stoichiometry; (b) changes in local current density in cells 1 and 2; plotted as a function of the normalized air channel length. Air stoichiometry in cells 1 and 2 of $\lambda_{air} = 1.2$.

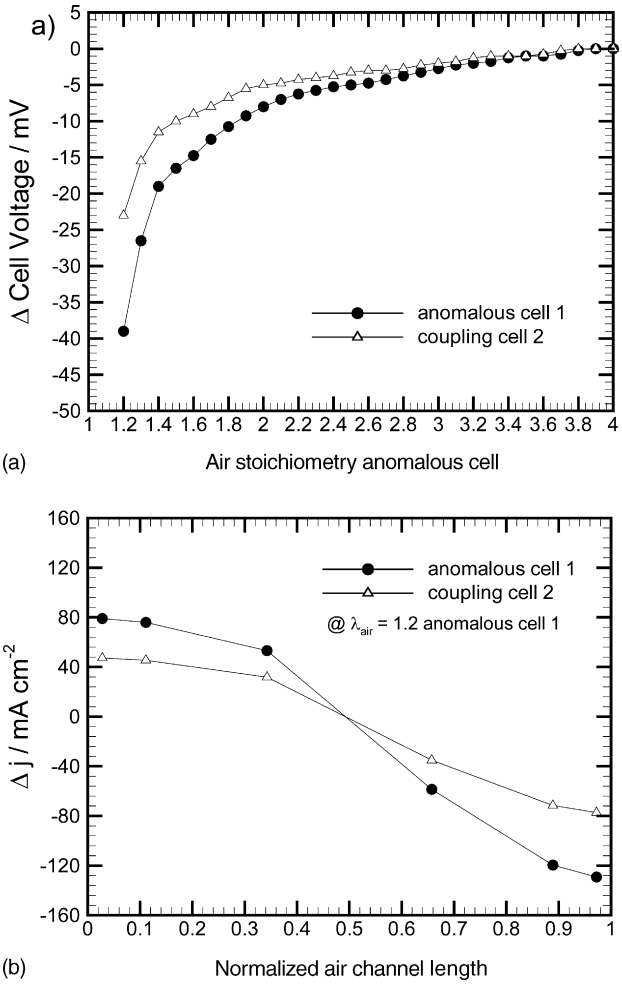

Fig. 4. 1 + 1-Cell stack. (a) Changes in cell voltage of the anomalous cell 1 and coupling cell 2; plotted as a function of the air stoichiometry in the anomalous cell 1; (b) changes in local current density in the anomalous cell 1 and coupling cell 2; plotted as a function of the normalized air channel length for an air stoichiometry $\lambda_{air} = 1.2$ in the anomalous cell 1.

in an increase in overall transport overpotential. On the other hand, reducing oxygen partial pressure leads to the evolution of a non-uniform current density distribution, which results in an overall increase of the activation overpotential [1,3].

3.2. Case 1 – emulation of air starvation – coupling to an immediate adjacent cell

The experimental setup allows for measurement of local current density only in peripheral cells in the stack. For this reason, in order to study the propagation of changes in local current density to an immediate adjacent cell, a first experiment was carried out using a 1 + 1-cell stack (see Table 1). The starvation of air at single cell level in the stack was emulated by gradually reducing air stoichiometry in one cell only (anomalous cell), while keeping the working conditions of the adjacent cell unaltered (coupling cell). Fig. 4a shows changes in cell voltage in the anomalous and coupling cells as a function of the air stoichiometry of the anomalous cell.

The results in Fig. 4a show that the performance of the anomalous cell follows the expected behavior when the air stoichiometry is reduced: a decrease in cell voltage. But also the second cell in the stack, the coupling cell shows qualitatively exactly the same performance behavior as the anomalous cell, even though the operating conditions are kept constant. Hence, a clear coupling between the cells takes place.

The question arises as to why the adjacent cell shows a coupled decrease in cell voltage? An examination of Fig. 4b clarifies this behavior. Here, changes in local current density in the anomalous and coupling cells along the air channel length are plotted for an air stoichiometry $\lambda_{air} = 1.2$ of the anomalous cell. The voltage coupling of the cells has an electronic origin: the changes in local current density in the anomalous cell (Fig. 4b) create a non-uniform feed of current into the bipolar plate. Due to the finite in-plane conductivity and thickness of the bipolar plate, the non-uniform distribution of current is homogenized only to a certain extent; hence, the current density pattern of the anomalous cell is impressed onto the adjacent cell (Fig. 4b). Changes in local current density in the coupling cell lead to a decrease in cell voltage because a current profile is impressed onto the coupling cell, which would not arise from its distribu-

tion of overpotentials (resistances). Consequently, the current takes a path through the electrochemical part of the cell which is non-optimal from the resistances point of view, leading to an increase in the sum of overpotentials.

For quantification of the propagation of changes in local current density a coupling factor was calculated. It is defined as the quotient between the sum of the deviations in local current density in the coupling cell with respect to the corresponding changes in the anomalous cell for air stoichiometries $\leq$2.0. Above this air stoichiometry the induced changes in cell voltage and local current density are small (<10 mV, <30 mA cm^{-2} respectively), consequently the relative changes carry a comparatively high error. The induced voltage changes in the coupling cell with respect to the changes in the anomalous cell where calculated in the same way.

With the given thickness, geometry, and conductivities of the bipolar plate, changes in the local current density of the anomalous cell propagate to an immediate adjacent cell for air stoichiometries $\leq$2.0 by a coupling factor of 0.64 ± 0.02; the induced change in cell voltage in the coupling cell is in the order of 0.59 ± 0.04 of the changes in the anomalous cell. These relatively strong coupling factors result from the relatively low thickness (3.1 mm) and low in-plane conductivity of the bipolar plate (100 s cm^{-1}). Thicker bipolar plates and/or plates with higher in-plane conductivities would yield lower coupling factors.

3.3. Case 2 – emulation of air starvation – coupling to non-immediate adjacent cells

In the previous chapter, it has been shown that a strong coupling phenomenon between immediate adjacent cells in a stack takes place when the local current density is strongly disturbed in one cell. Logically the question arises as to how far and to which extent this anomaly will propagate further into the stack? To answer this question an experiment with a three-cell stack was performed (1 + 2-cell stack, see Table 1), in which the air starvation anomaly was emulated in the first cell, while keeping the working conditions of the two adjacent cells constant. Again the cell voltage of each cell was simultaneously recorded while measurement of local current density was realized in the peripheral cells of the stack; these being cells 1 and 3, correspondingly.

The changes in cell voltage also spread significantly to cell 3 as it can be seen in Fig. 5a. Again, the reason for the changes in cell voltage is due to the propagation of changes in local current density originating in the anomalous cell and passed over first to the immediate adjacent cell 2 and then to cell 3, as it can clearly be seen in Fig. 5b. Because the experimental setup does not allow for measuring the local current density in cells located in the middle of the stack, the current density pattern registered in the anomalous cell in the 1 + 1 stack is shown to illustrate the diminishment in the coupling amplitude to a non-immediate adjacent cell.

The coupling factors of cell voltage and local current density changes induced by the anomalous cell 1 onto the coupling cells 2 and 3 as a function of the air stoichiometry are shown in

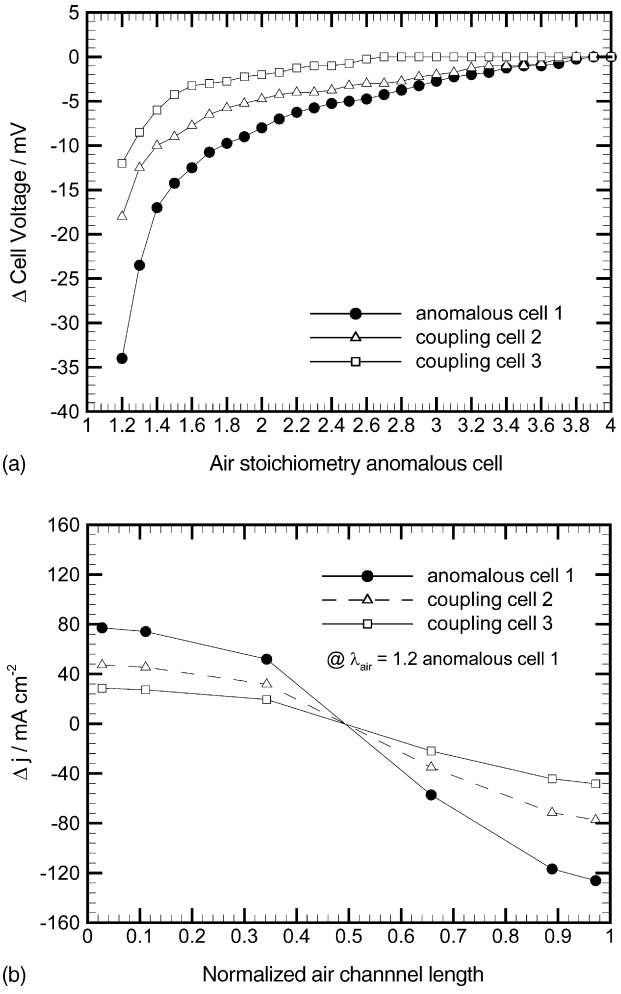

Fig. 5. 1 + 2-Cell stack. (a) Changes in cell voltage of the anomalous cell 1 and coupling cells 2 and 3, respectively; plotted as a function of the air stoichiometry in the anomalous cell 1; (b) changes in local current density in the anomalous cell 1 and coupling cells 2 and 3; plotted as a function of the normalized air channel length for an air stoichiometry $\lambda_{air} = 1.2$ in the anomalous cell 1 (data for the coupling cell 2 were obtained in a 1 + 1-cell stack).

Fig. 6a and b. The data is shown for air stoichiometries $\leq$2.0. For cell 2 in Fig. 6b, the values obtained from the measurements in the 1 + 1-cell stack are shown. The changes in local current density originating in the anomalous cell propagate to an immediate adjacent cell by a coupling factor of 0.64 ± 0.02 and to a second cell by a factor of 0.40 ± 0.04. As for the changes in cell voltage, an immediate adjacent cell couples to the changes in the anomalous cell with a factor of 0.59 ± 0.04, while the coupling factor for the voltage changes in the second cell are in the order of 0.32 ± 0.05. From these values a quadratic relation in the attenuation of changes in local current density passed from cell to cell becomes apparent for the investigated bipolar plate properties. Therefore, the performance of cells located in fourth position adjacent to an anomalous cell is not expected to be affected significantly, since the coupled changes in local current density would be in the order of a few per cent only. From the relation in the propagation of voltage changes, it can also be calculated that a fourth cell adjacent to an anomalous cell will

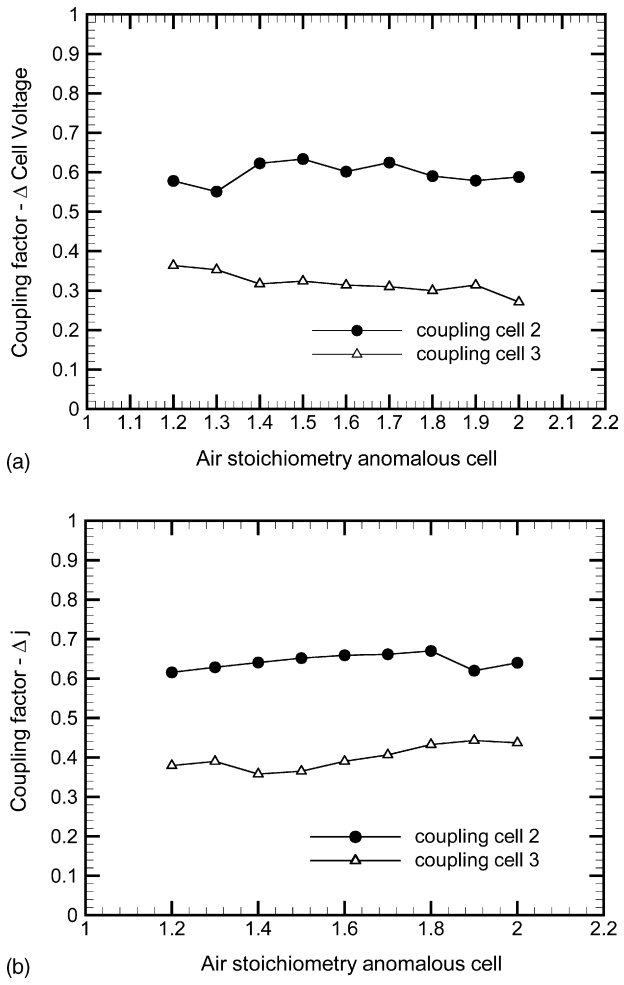

Fig. 6. Coupling factors as function of the air stoichiometry in the anomalous cell 1: (a) for changes in cell voltage in the coupling cells 2 and 3; (b) for changes in local current density in the coupling cells 2 and 3. Calculated with reference to the corresponding changes in the anomalous cell 1.

show practically no changes in cell voltage. As outlined in the previous chapter, the extent of coupling is dictated by the bipolar plate thickness and in-plane conductivity.

In order to reduce coupling effects, thicker plates of the same material could be employed. This of course is unwanted because it would increase stack weight and volume. Alternatively, the in-plane conductivity of the plate material needs to be increased to reduce coupling effects. This reasoning shows that not only the bipolar plate through-plane conductivity is of high importance, but also its in-plane conductivity for optimization of performance and reliability of a PEFC stack.

3.4. Case 3 – emulation of thermal losses – coupling to an immediate adjacent cell

A commonly encountered phenomenon in fuel cell stacks is that the performance of cells located in the periphery of the stack (i.e. first or last cell) may differ from the average performance of the rest of the cells. These cells can experience increased thermal losses because of their peripheral location in the stack which makes them more susceptible to temperature variations which could affect their performance in relation to other cells in the stack.

To investigate the propagation of performance changes originating from a thermally anomalous cell to an immediate adjacent cell, experiments with a 1 + 1-cell stack were carried out. To emulate increased thermal losses in a peripheral cell, the inlet temperature of the coolant liquid in cell 1 (anomalous cell) was gradually decreased, while keeping the inlet coolant temperature of the adjacent cell 2 (coupling cell) constant. Table 2 gives the temperature of the coolant in both cells, measured at the inlet and outlets of each cell. Such big differences in working temperature between the peripheral cells and the set temperature for the stack are not likely to be encountered in reality, but were chosen in order to maximize the observable effects.

With the experimental setup used for the presented case, thermal losses in cell 1 can be emulated as originating from the periphery of the stack because the coolant temperature in the external side of cell 1 can be controlled independently (see Fig. 1). To account for possible thermal losses in cell 2 (in the 1 + 1-cell stack both cells are obviously peripheral cells) an external heating device, set to the temperature of cell 2, was placed on the supporting metallic endplate, to simulate for the presence of a continuing stack behind cell 2. Heat transport from cell 2 to cell 1 through the bipolar plate causes an increase in coolant temperature in cell 1. However, the temperature of cell 2 remains practically constant as it can clearly be seen from its inlet and outlet coolant temperatures (see Table 2) because additional heat is fed in by the external heating.

As can be seen in Fig. 7a, the anomalous cell experiences evident performance changes depending on its working temperature. Conversely, and very surprisingly indeed, the performance of the adjacent cell is not affected at all by the anomaly in the working temperature of the anomalous cell. Obviously, the question arises as to how this can be possible, considering the substantial changes in cell voltage observed in the anomalous cell. Fig. 7b gives an explanation to this question. It can be seen that, even for the lowest experimentally realized operating temperature in the anomalous cell (inlet and outlet coolant temperatures of 30 and 56 °C, respectively, see Table 2), changes in

Table 2
Inlet and outlet coolant temperature from the cells 1 and 2 in the 1 + 1-cell stack for case 3

Location of coolant temperature measurement	Cell 1 coolant temperature (°C)	Cell 2 coolant temperature (°C)
Inlet	71	72
Outlet	71	72
Inlet	61	72
Outlet	67	72
Inlet	51	72
Outlet	64	71
Inlet	41	72
Outlet	60	71
Inlet	30	72
Outlet	56	70

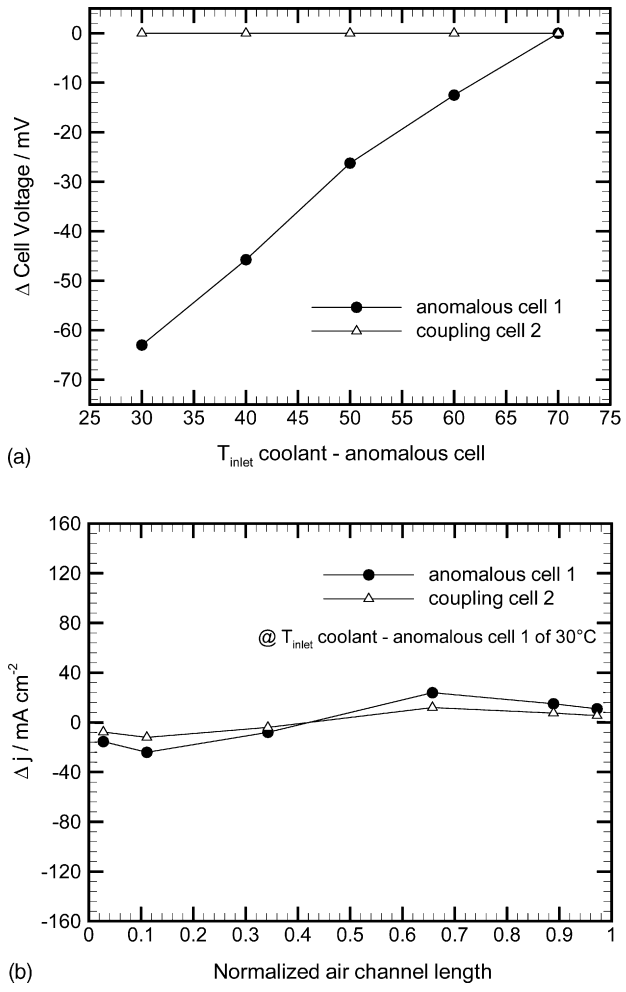

Fig. 7. 1 + 1-Cell stack. (a) Changes in cell voltage in the anomalous cell 1 and coupling cell 2; plotted as a function of the coolant inlet temperature T_{inlet} of the anomalous cell 1; (b) changes in local current density in the anomalous cell 1 and coupling cell 2; plotted as a function of the normalized air channel length for an inlet coolant temperature $T_{inlet} = 30\,^{\circ}C$ in the anomalous cell 1.

local current density in the anomalous cell are relatively small (<25 mA cm^{-2}); consequently, induced changes in local current density in the adjacent cell are minor. Variations in local current density registered in the anomalous cell depend upon location of the segments with respect to the coolant in- and outlets. The reactant gases were fed fully humidified in order not to induce humidification related changes of the membrane resistance and therefore to exclude any influence on the local current density. In the case of low humidification of the reactant gases, changes in cell temperature will affect the local water content of the membrane (i.e. its conductivity) and as a consequence bigger changes in local current distribution will evolve, which can propagate to adjacent cells.

The drastic voltage changes in the anomalous cell are due to changes in the activation overpotential and membrane conductivity. Since the temperature of the adjacent cell is kept constant (see Table 2) and the electronic coupling of the cells is minimal, as a result, the voltage of the adjacent cell remains practically unchanged. Finally, attention has to be drawn to the fact that, without measurement of local current density in both cells, an explanation for this phenomenon would not be that straightforward.

The findings of the above experiment with a 1 + 1-cell stack were confirmed in an experiment carried out with a three-cell stack (1 + 2) emulating thermal losses in cell 1. As expected, also in this experiment no propagation of performance changes due to a thermal anomaly in cell 1 to the adjacent cells was observed.

4. Conclusions

In a fuel cell stack, individual cells may show an anomalous behavior with reference to their stand-alone performance because of differences in the operating conditions at single cell level: these differences can arise due to variations in manufacturing tolerances, differences in reactant flow and temperature as well as location in the stack.

Performance changes originating from anomalies inducing considerable variations in local current density, such as air starvation, can propagate even to non-immediate adjacent cells through the stack. The coupling has an electronic character and takes place via the common bipolar plate. In the performed experiments a quadratic relation in the attenuation of the changes in local current density passed from cell to cell has been observed. Hence, a complete homogenization of the local current changes originated in an anomalous cell does not take place in the common bipolar plate via in-plane currents due to its finite conductivity and thickness. As a consequence, a local current density profile is impressed onto the coupling cells, which would not arise from their distribution of overpotentials under their individual working conditions. Consequently, the current takes a path through the electrochemical part of the cell which is non-optimal from the resistances point of view, leading to an increase in the sum of overpotentials and ultimately a decrease in cell voltage.

Consequently, anomalies which do not induce considerable changes in local current density in an anomalous cell, such as temperature differences when the gases are fed well humidified, do not propagate to adjacent cells.

Acknowledgement

The authors would like to thank T. Gloor for various contributions to this work.

References

[1] D.J.L. Brett, S. Atkins, N.P. Brandon, V. Vesovic, N. Vasileiadis, A.R. Kucernak, Electrochem. Commun. 3 (2001) 628–632.
[2] F.N. Büchi, A.B. Geiger, R.P. Neto, J. Power Sources 145 (2005) 62–67.
[3] A.A. Kulikovsky, A. Kucernak, A.A. Kornyshev, Electrochim. Acta 50 (2005) 1323–1333.
[4] A.B. Geiger, R. Eckl, A. Wokaun, G.G. Scherer, J. Electrochem. Soc. 151 (2004) A394–A398.
[5] I.A. Schneider, H. Kuhn, A. Wokaun, G.G. Scherer, J. Electrochem. Soc. 152 (2005) A2092–A2103.
[6] D. Kramer, E. Lehmann, G. Frei, P. Vontobel, A. Wokaun, G.G. Scherer, Nucl. Instrum. Methods A 542 (2005) 52–60.

[7] H. Nishikawa, R. Kurihara, S. Sukemori, T. Sugawara, H. Kobayasi, S. Abe, T. Aoki, Y. Ogami, A. Matsunaga, J. Power Sources 155 (2006) 213–218.
[8] G.S. Kim, J. St-Pierre, K. Promislow, B. Wetton, J. Power Sources 152 (2005) 210–217.
[9] F.N. Büchi, A. Tsukada, P. Rodatz, O. Garcia, M. Ruge, R. Kötz, M. Bärtschi, P. Dietriech, Proceedings of the Fuel Cell World, Lucerne, Switzerland, July 1–5, 2002, pp. 218–231.
[10] M. Ruge, Doctoral Thesis No. 14901, ETH Zürich, Switzerland, 2002.
[11] M. Ruge, F.N. Büchi, Proceedings of the Energy and Electrochemical Processes for a Cleaner Environment of the 200th Meeting of the Electrochem. Soc., 2001, pp. 165–173.
[12] M. Santis, Doctoral Thesis, ETH Zürich, Switzerland, to be published 2006.